Journal of Drug Targeting

http://informahealthcare.com/drt
ISSN: 1061-186X (print), 1029-2330 (electronic)

J Drug Target, Early Online: 1–15
 DOI: 10.3109/1061186X.2015.1025077

informa
healthcare

ORIGINAL ARTICLE

Co-delivery of doxorubicin and siRNA for glioma therapy by a brain targeting system: angiopep-2-modified poly(lactic-co-glycolic acid) nanoparticles

Lei Wang*, Yongwei Hao*, Haixia Li, Yalin Zhao, Dehui Meng, Dong Li, Jinjin Shi, Hongling Zhang, Zhenzhong Zhang, and Yun Zhang

School of Pharmaceutical Sciences, Zhengzhou University, Zhengzhou, PR China

Abstract

It is very challenging to treat brain cancer because of the blood–brain barrier (BBB) restricting therapeutic drug or gene to access the brain. In this research project, angiopep-2 (ANG) was used as a brain-targeted peptide for preparing multifunctional ANG-modified poly(lactic-*co*-glycolic acid) (PLGA) nanoparticles (NPs), which encapsulated both doxorubicin (DOX) and epidermal growth factor receptor (EGFR) siRNA, designated as ANG/PLGA/DOX/siRNA. This system could efficiently deliver DOX and siRNA into U87MG cells leading to significant cell inhibition, apoptosis and EGFR silencing *in vitro*. It demonstrated that this drug system was capable of penetrating the BBB *in vivo*, resulting in more drugs accumulation in the brain. The animal study using the brain orthotopic U87MG glioma xenograft model indicated that the ANG-targeted co-delivery of DOX and EGFR siRNA resulted in not only the prolongation of the life span of the glioma-bearing mice but also an obvious cell apoptosis in glioma tissue.

Keywords

Blood–brain barrier, brain delivery, DOX, drug delivery, siRNA

History

Received 7 January 2015
Revised 25 February 2015
Accepted 27 February 2015
Published online 9 April 2015

Introduction

It is well known that it is very challenging to treat brain cancer because of the blood–brain barrier (BBB) restricting therapeutic drug or gene to access the brain [1]. With wide application of nanotechnology in medicine, there are increasing high expectations for the delivery of therapeutics to the brain for treating glioma [2].

Poly(lactic-*co*-glycolic acid) (PLGA) has been widely used in drug delivery system in recent years owing to its outstanding biocompatibility and biodegradability [3,4]. In America, FDA has formally approved PLGA as a pharmaceutical excipient. Therefore, a number of PLGA-based nanoparticles (NPs) as drug delivery systems have been reported [5].

Epidermal growth factor receptor (EGFR) amplification, over-expression and mutation are the common molecular events in oncogenesis of glioblastomas [6]. Thus, targeted therapy against EGFR is a good choice for treating glioma [7]. RNA interference (RNAi) is a simple, rapid and economical alternative to current other gene targeting approaches both *in vitro* and *in vivo* [8]. However, constructing efficient delivery system is still the most challenging task in the development of RNAi as an extensive therapeutic platform [9]. Meanwhile, the molecular complexity of cancer indicates that the use of a single therapeutic agent may not be sufficient to stop the progression of most cancers [10]. As an emerging approach, the combination of gene therapy and chemotherapy offers hope for the treatment of glioma [11,12]. Recently, many co-delivery systems carrying chemotherapeutic drug and gene have been reported [13–15]. Wang et al. constructed a multifunctional magnetic NP system for the treatment of glioblastoma, which exhibited potential application for glioma therapy [16]. Accumulating studies have shown that PLGA-based NPs may be a new choice of gene and drug carriers [17,18]. However, there is more room for the current PLGA-based NPs to improve in delivery efficiency and therapeutic effect, and the co-delivery of EGFR siRNA and doxorubicin (DOX) by a PLGA carrier for glioma therapy has not yet been reported before.

Although, simultaneous delivery of both drug and gene can be achieved by NPs, it is powerless to home them specifically to brain tumors. Therefore, a targeting ligand is necessary for glioma therapy. Researches had reported that brain capillary endothelial cells and malignant tumor cells over-expressed low-density lipoprotein receptor-related protein-1 (LRP-1) [19–21]. Angiopep-2 (ANG), a novel brain targeting peptide, has been proved to efficiently bind to LRP-1 to assist drug delivery systems including NPs to cross the BBB [19,20]. GRN1005, a conjugate of one molecule of ANG and three

*These authors contributed equally to this work.

Address for correspondence: Prof. Zhenzhong Zhang and Prof. Yun Zhang, School of Pharmaceutical Sciences, Zhengzhou University, 100 Kexue Avenue, Zhengzhou, Henan Province 450001, PR China. Tel: +86 371 67781910. Fax: +86 371 67781908. E-mail: zhangzz08@126.com (ZZ); zhang_yun@ymail.com (YZ)

molecules of paclitaxel, can actively penetrate into the brain compartment by targeting LRP-1, which was under Phase I clinical trial in the US for the treatment of recurrent glioma [22]. Thus, ANG can not only enhance the transport of NPs across the BBB but also increase the accumulation of therapeutic drugs in the brain tumor cells.

In the present study, we designed a multifunctional ANG-modified PLGA NPs loaded with both DOX and EGFR siRNA, which is designated as ANG/PLGA/DOX/siRNA. The brain targeting peptide ANG was conjugated with NPs through chitosan. DOX was loaded in the core section of the NPs, while the EGFR siRNA was adsorbed by NPs through electrostatic adherence. This new formulation was well characterized, and the *in vitro* cellular uptake and the combination anticancer effect of DOX and EGFR siRNA on U87MG cells were studied to determine the applicability of the drug delivery system in glioma therapy. Besides, brain targeting of PLGA NPs loaded with coumarin-6 and the anti-glioma effect were also investigated *in vivo*.

Materials and methods

Materials

PLGA (lactide/glycolide = 50:50, MW: 17 000 Da) was purchased from Jinan Daigang Biomaterial Co., Ltd (Jinan, China). Chitosan (deacetylation degree ≥95%, viscosity 20–30 mPa s) was purchased from Qingdao Alfrolong Bitotech Co., Ltd (Qingdao, China). Doxorubicin hydrochloride (DOX, purified >98%) was purchased from Dalian Meilun Biotech. Co., Ltd (Dalian, China). EGFR siRNA (sense 5′-GUGUGUAACGGAAUAGGUATT-3′; anti-sense: 5′-UACCUAUUCCGUUACACACTT-3′) was produced by Genepharma (Shanghai, China). ANG (TFFYGGSRGKPN NFKTEEYC, Mw = 2404.6 Da) was synthesized by CL. (Xian) Bio. Scientific Co., Ltd. U87MG cells were obtained from Chinese Academy of Sciences Cell Bank (Catalog NO. Tchu138). 3-Maleimido propionic acid *N*-hydroxy succinimide ester (NHS-Pr-Mal) was purchased from Sigma-Aldrich, Inc. (St Louis, MO). The water used was pretreated with the Milli-Q Plus System (Millipore Corporation, Bedford, MA). All other chemicals were of analytical grade and used without further purification. Experimental animals were purchased from the Henan Laboratory Animal Center and all the *in vivo* experiments were performed in accordance with the protocols evaluated and approved by the Ethical Committee of Zhengzhou University.

Synthesis and characterization of ANG–chitosan

The conjugation of ANG to the chitosan (ANG–chitosan) was performed as depicted in Figure 1(A). In brief, chitosan was dissolved in 20% acetic acid solution at a concentration of 2 mg/mL; the solution was adjusted to pH 6.0 by gradual addition of sodium hydroxide (0.1 M). About 25 mg of NHS-Pr-Mal was then added to the chitosan solution at 40 °C. The reaction was performed for 48 h under the nitrogen atmosphere. The reaction solution was then dialyzed against deionized water for 48 h using a dialysis bag with a Mw cut-off of 12 kDa (Spectrum Laboratories). Finally, 1 mg of ANG was added to the reaction solution followed by a pH adjustment to 7.4, and then the reaction was continued for 12 h at 35 °C. The synthesized product (ANG–chitosan) was dialyzed against deionized water for 48 h, and then frozen at −80 °C. The obtained product was stored at −20 °C for future use.

Both chitosan and ANG–chitosan were grounded with potassium bromide (KBr) and crushed to form a uniform fine power in an agate mortar followed by compression to get a thin pellet, respectively. An FT-IR Spectrometer (Nicolet Is10 spectrometer, Thermo Scientific, Waltham, MA) then scanned the pellet.

The ANG–chitosan was dissolved in a mixed solvent comprised of D_2O and CD_3COOD (1:1, v/v) and then characterized by ^1H NMR spectrum (Bruker DMX-500 spectrometer, Rheinstetten, Germany).

The relative amount of ANG grafted to chitosan was measured by the bicinchoninic acid (BCA) protein assay as per the manufacturer's instruction.

Preparation of NANG/PLGA/DOX and ANG/PLGA/DOX NPs

The ANG-targeting PLGA NPs loaded with DOX (ANG/PLGA/DOX) and non-ANG-targeting PLGA NPs loaded with DOX (NANG/PLGA/DOX NPs) were prepared by nano-precipitation [23]. Briefly, DOX and PLGA were simultaneously dissolved in the mixed organic solvent of methanol and acetone (1:3, v/v) at a final concentration of 3 and 10 mg/mL, respectively. The water phase was prepared by dissolving bovine serum albumin (BSA, Roche, biotechnology Grade, Purify ≥98%), chitosan or ANG–chitosan in diethypyrocarbonate (DEPC) treated water at a concentration of 10 mg/mL (BSA) and 1.5 mg/mL (chitosan or ANG–chitosan), respectively. In order to dissolve chitosan or ANG–chitosan completely, the pH of the water phase was adjusted to 6.0. After that, an aliquot of 1 mL of organic phase was added to 4 mL of water phase gradually under a stirring condition at 25 °C, followed by ultrasonication (200 W, 20 times) with a JV92 ultrasonic cell disruption system (Ninbo Scientz Biotechnology Co., Ltd., Zhejiang, China). The organic solvents were removed by continuous stirring at room temperature for 24 h. Coumarin-6-loaded PLGA NPs for *in vivo* studies were similarly prepared, except that DOX was replaced with coumarin-6 in the formulation.

Preparation of NANG/PLGA/DOX/siRNA and ANG/PLGA/DOX/siRNA NPs

A predetermined amount of EGFR siRNA was added to DEPC-treated vials, which contained appropriate amount of NANG/PLGA/DOX NPs or ANG/PLGA/DOX NPs. The complexation was completed by incubation for 30 min at 25 °C before use.

Determination of siRNA complexation by gel retardation assay

The binding degree between siRNA and ANG/PLGA/DOX NPs was estimated by agarose gel electrophoresis. Complexation of ANG/PLGA/DOX NPs with siRNA was induced at various weight ratios ranging from 15:1 to 90:1.

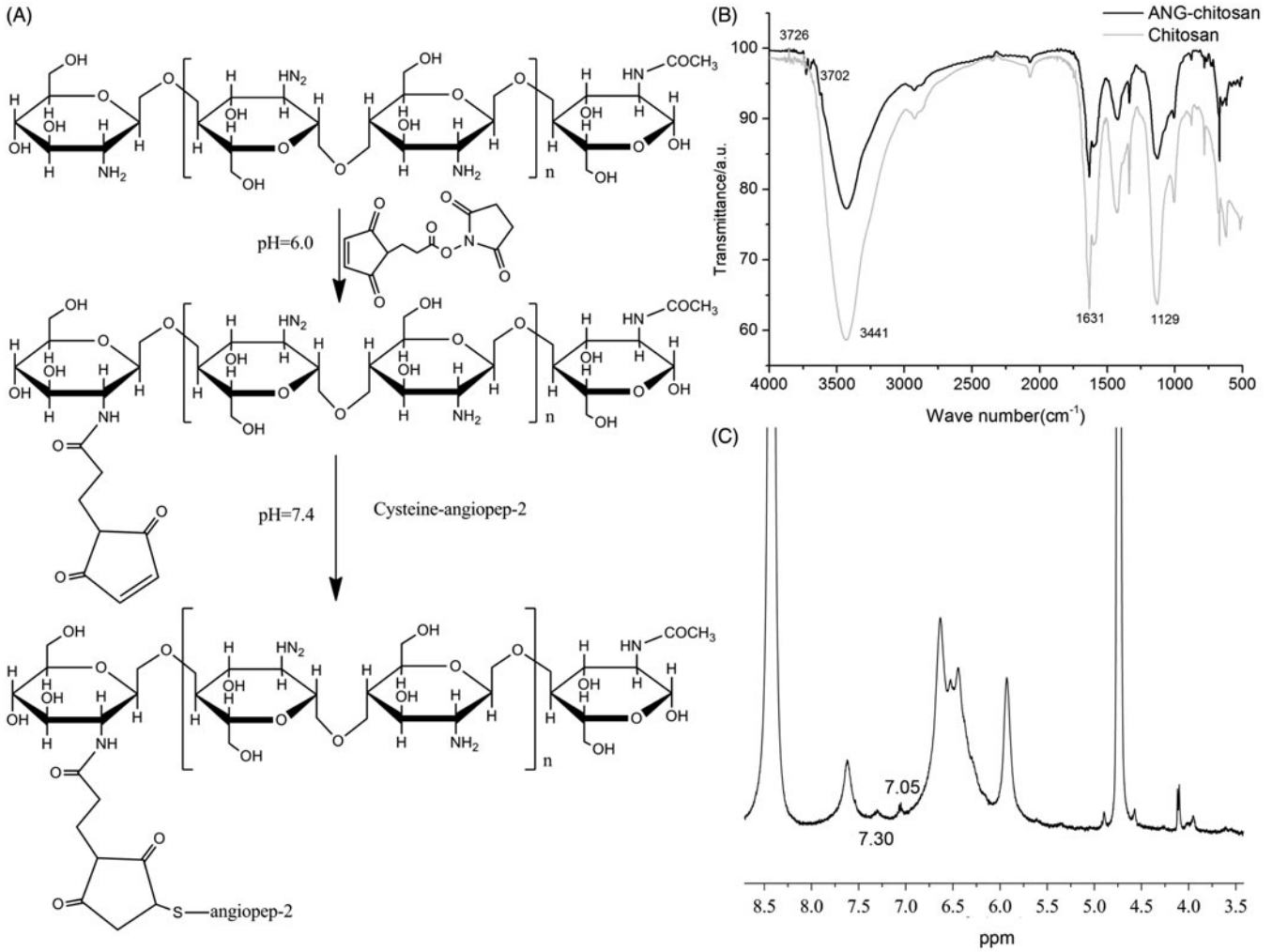

Figure 1. Synthetic route of ANG–chitosan and characterization. (A) Synthetic route of ANG–chitosan; (B) FT-IR spectrum of chitosan and ANG–chitosan; (C) ^{1}H NMR spectrum of ANG–chitosan.

The complexes were loaded onto 1% agarose gels with Goldview™ and run with TAE buffer solution (40 mM Tris-HCl, 1 v/v% acetic acid and 1 mM EDTA) at 100 V for 15 min. Retardation of siRNA mobility was revealed by irradiation with UV light.

Characterization of DOX-loaded NPs

Determination of size distribution and zeta potential

A sample of 100 µL of ANG/PLGA/DOX/siRNA NPs was diluted with ultrapure water to 2 mL. The size distribution and zeta potential of the NPs were evaluated at 25 °C by a Nano ZS-90 (Malvern Instruments, Worcestershire, UK) based on quasi-elastic light scattering.

Determination of encapsulation efficiency of DOX

Ultracentrifugation was employed to determine the encapsulation efficiency of DOX. A sample of 500 µL of NPs was placed into an ultra-15 centrifugal filter device with a Mw cut-off of 10 kDa to centrifuge at 10 000 *g* for 1 h to separate DOX-loaded NPs from free DOX. A standard absorbance–concentration calibration curve was plotted after measuring a series of standard concentrations of DOX dissolved in water. The spectrophotometric qualification was achieved by measuring the absorbance at 479 nm using an UV–Vis spectrophotometer (Shimadzu, Tokyo, Japan). Encapsulation ratio was determined by the following formula:

$$\text{Encapsulation ratio } \% = \frac{M_{\text{DOX-prep}} - M_{\text{DOX-supernatant}}}{M_{\text{DOX-prep}}} \times 100$$

where $M_{\text{DOX-prep}}$ is the initial amount of DOX for preparation and $M_{\text{DOX-supernatant}}$ is the DOX recovered from the supernatant, which represents the free drug.

In vitro *release study*

ANG/PLGA/DOX/siRNA NPs, NANG/PLGA/DOX/siRNA NPs and free DOX were placed in screw capped dialysis bags with a Mw cut-off of 14 kDa, and then dipped in 30.0 mL of phosphate-buffered saline (PBS, pH 7.4), respectively. Then, they were placed in an orbital shaker bath, followed by shaking horizontally at 100 rpm at 37 °C. At the specified time intervals, samples were drawn from the solution, and the same volume of fresh PBS was replenished. The concentration of DOX released from ANG/PLGA/DOX NPs, NANG/PLGA/DOX NPs and free DOX was quantified by high-pressure liquid chromatography (Agilent 1200, Santa

Clara, CA). The chromatographic parameters and conditions were set as follows: an Inertex-C18 column (150 mm × 4.6 mm, 5.0 μm); column temperature was set at 30 °C; mobile phase was methanol/acetonitrile/0.02 M ammonium dihydrogen phosphate/acetic acid (52:5:42.4:0.6, v/v); The excitation wavelength and emission wavelength were set at 505 and 555 nm for fluorescence detector; and injection volume was 20 μL.

Differential scanning calorimetry (DSC)

The physical state of DOX entrapped in the NPs was characterized by DSC. A sample of 5–10 mg of DOX, PLGA, freeze-dried ANG/PLGA/DOX NPs, freeze-dried blank ANG/PLGA NPs or a mixture of freeze-dried blank ANG/PLGA NP and DOX (DOX:blank NPs = 1:8) was placed in a standard aluminium pan with a lid. The heating rate was set at 10 °C/min from 30 to 350 °C in a differential scanning calorimeter (Shimadzu DSC-60A, Kyoto, Japan).

Cell culture and uptake

U87MG cells were cultured at 37 °C in a humidified 5% CO_2 atmosphere. MEM culture medium contained 10% Hyclone® fetal bovine serum (FBS, Hyclone, Thermo Fisher Co., Logan, UT), 0.1 mg/mL streptomycin and 100 U/mL penicillin (Beijing Dingguo Changsheng Biotech Co. Ltd., China).

U87MG cells were plated at a concentration of 2.5×10^5 per well in 6-well plates (Coring Inc., Corning, NY) with a glass coverslip in each well. After 24 h incubation, the adherent cells were incubated with different formulations at a concentration of 50 nM FAM-labelled siRNA or 3.6 μM DOX in medium without serum. After incubation for 5 h, the cells were gently washed with PBS, followed by counterstaining with 4′,6-diamidino-2-phenylindole (DAPI, 1 μg/mL) for 15 min to stain the cell nuclei, and then imaged with a confocal laser scanning microscope (Olympus Flowview V1000, Tokyo, Japan).

The DOX and FAM-labelled siRNA content in cells were determined by a flow cytometry (Accuri C6, BD, Franklin Lakes, NJ) [24]. The cells were trypsinized and collected, washed with PBS. After resuspension in 0.5 mL of PBS, cells were analyzed by flow cytometry with a 488 nm laser for FAM-siRNA and DOX excitation. The fluorescence from DOX and FAM-siRNA were measured with a 575 or 525 nm filter, respectively. Cells without incubation with drug were detected as a control for background calibration. The data were analyzed by using FlowJo software, Version 7.6.1 (Tree star Inc., Stanford, UK).

Cytotoxicity and cell viability assay

U87MG cells were seeded into 96-well culture plates at a density of 5×10^3 per well in 200 μL of MEM culture medium containing 10% FBS, 0.1 mg/mL streptomycin and 100 U/mL penicillin, and then cultured at 37 °C.

After a 24 h incubation, the culture medium was replaced by blank PLGA NPs, free DOX, ANG/PLGA/DOX NPs or NANG/PLGA/DOX NPs with different DOX concentrations, respectively. We evaluated the co-delivery of DOX and siRNA by ANG-targeting PLGA NPs and non-ANG-targeting PLGA NPs at different concentrations of DOX and a fixed siRNA concentration of 50 nM, which were represented by ANG/PLGA/DOX/siRNA and NANG/PLGA/DOX/siRNA, respectively. In this section, the serum-free growth medium was used. After a 5 h incubation, the growth medium in each well was substituted with the fresh serum-containing MEM medium. After the treated cells were cultured for extra 24 or 48 h, the sulforhodamine B assay (SRB) was used to determine the cell viability. All measurements were performed in triplicate.

Real-time RT-PCR analysis

The cellular level of EGFR mRNA was evaluated using qRT-PCR (quantitative real-time polymerase chain reaction). U87MG cells were seeded in 96-well plates at a density of 5×10^3 per well. The cells were cultured for 24 h before use. The culture medium was removed and replaced by 2 mL serum-free MEM containing different NPs. The final concentration of EGFR siRNA was 50 nM. After 5 h incubation, the medium was substituted with complete MEM medium followed by incubation for additional 48 h. Then, the cells were collected and the total RNA was extracted using RNAiso Plus as per the manufacturer's instruction. Synthesis of cDNA was gained by RT with oligo dT priming and the reverse transcription system for TR-PCR. The real-time PCR was completed with SYBR Green qPCR Kit Master Mix. PCR was performed according to an improved three-step amplification method (95 °C for 10 s, then 58 °C for 15 s and 95 °C for 15 s, 45 cycle) followed by a melting curve to demonstrate the production of a single PCR product. The threshold cycle number (CT) was analyzed for hEGFR and β-actin using Eco™ Software v3.1.7.0. β-Actin gene was selected as an inner control. For hEGFR, the sense and anti-sense primer sequences are 5′-CGTGCCCTGATGGATGA-3′ and 5′-CCACGGTGGAATTGTTGCTG-3′, respectively. For β-actin, the sense and anti-sense primer sequences are 5′-AGAGCTACGAGCTGCCTGAC-3′ and 5′-AGCACTG TGTTGGCGTACAG-3′, respectively. Relative gene expression of hEGFR was calculated with the 2-(ΔΔCT) method as described previously [25].

Apoptosis assay

U87MG cells were cultured in 6-well plates at a density of 2.5×10^5 per well. After the cells were cultured for 24 h, the different preparations in serum-free culture medium were added. After a 5 h incubation, the cell culture medium in each well was substituted with the same volume of serum-containing MEM medium, and the cells were further incubated for 24 h. The staining of the cells was performed with Annexin V-FITC/PI as per manufacturer's instruction. Cells were collected for flow cytometry. Flowjo software, Version 7.6.1 (Tree star Inc., Stanford, UK) was applied to analyze the data.

Brain delivery via tail vein injection

After intravenous injection of coumarin-6-loaded PLGA NPs for 1, 2 or 3 h, the mice were sacrificed and their whole brains were collected and frozen in OCT medium. Cryosection of

the brain tissues was carried out and the slides were stained with DAPI (1 μg/mL) for 15 min followed by observation with a microscope (Nikon Eclipse 50, Japan). The representative pictures of striatum were recorded, respectively.

Pharmacokinetics and biodistribution studies

To further assess the biodistribution and brain targeting ability of the DOX-loaded NPs, we randomly divided mice into three groups. The mice were administered intravenously a single dose of DOX (3 mg/kg) in the form of DOX solution or DOX-loaded NPs. After 0.083, 0.25, 0.5, 1, 2, 3 h of injection, blood samples were collected from mice's eyes *via* retro orbital bleeding in each group. At 3 h after the administration, tissues/organs were harvested, weighted and homogenized in saline.

The concentrations of DOX from plasma and tissues/organs were measured by HPLC (Agilent 1200) as described previously [26,27]. The pharmacokinetic parameters were calculated using non-compartment analysis with PK solver (China Pharmaceutical University, Nanjing, China).

In vivo efficacy of drug-loaded NPs

Anesthesia of BALB/c nude mice was induced by an initial subcutaneous injection of diazepam (1 mg/kg) followed by an intraperitoneal injection of pentobarbital sodium (40 mg/kg). A burr hole was drilled 3 mm to the right of midline and 1 mm anterior to bregma. U87MG cells were dispersed in serum-free MEM containing 1.2% carboxymethylcellulose. Ten microliters of cell suspension containing 5×10^5 cells were slowly injected into the right striatum at a depth of 3.5 mm over 5 min [7]. On the 10th, 13th and 16th day after the implantation, the model mice were repeatedly treated by intravenous administration of saline, DOX, NANG/PLGA/DOX, ANG/PLGA/DOX, NANG/PLGA/DOX/siRNA or ANG/PLGA/DOX/siRNA at a dose of 3 mg/kg of DOX and 1.2 mg/kg of siRNA. At 25 days after the implantation, one mouse was randomly picked from each group and sacrificed to collect brain and heart. The collected brain samples were sliced into coronal sections using a sliding microtome. The slices of brain were stained with Nissl to roughly estimate and compare the tumor size because Nissl stains glioma tissue blue. The slices of heart were stained with haematoxylin and eosin (H&E) using routine protocols. The remaining six mice in each group were saved and monitored for survival times. Paraffin tissue sections of the tumors were prepared from the sacrificed mice under moribund conditions. Apoptotic cell in glioma tissue was evaluated by TUNEL assay using an *in situ* cell apoptosis detection kit as per the manufacturer's instructions before observation under a microscope.

Data analysis

Data were analyzed by using an F-test with subsequent Student's t-test (equal variance) for comparison between two different groups. For three or more groups, ANOVA was performed followed by Dunnett post test. Survival curves were drawn with the Kaplan–Meier method and the survival period was analyzed by using a nonparametric log-rank test. Results were considered statistically significant at $p < 0.05$. All data reported are mean value ± S.D., unless otherwise noted.

Results and discussion

Synthesis and characterization of ANG–chitosan

Chitosan has been a non-toxic and efficient vector for *in vitro* gene transfection and *in vivo* gene delivery [28]. In order to improve the targeting ability, some targeting groups were grafted on chitosan, including TAT [29] and folate [30]. In this study, ANG-modified chitosan (ANG–chitosan) was synthesized as depicted in Figure 1(A).

The FT-IR spectra of chitosan in Figure 1(B) illustrated three bands at 3441, 1631 and 1129 cm^{-1}, which corresponded to O–H vibrations, C=O vibrations and C–O–C vibrations of chitosan molecule. Compared with the spectra of chitosan, the characteristic peaks of NH_2 for surface external bending between 500 and 900 cm^{-1} in ANG–chitosan had been strengthened, indicating the existence of ANG. Moreover, the new peaks at 3726 and 3702 cm^{-1} may also explain the success of ANG grafting to chitosan.

In ^1H NMR spectrum (Figure 1C), the solvent peaks of D_2O and CD_3COOD were found at 4.7 and 8.43 ppm, respectively. The characteristic unit peak of benzene coming from some amino acids that composed ANG presented the corresponding peaks at 7.05 and 7.30 ppm, suggesting the existence of the conjugate structure of ANG-modified chitosan.

The relative amount of ANG grafted to chitosan was measured by the BCA protein assay. The result showed that about 23.48 μg of ANG was grafted to 1 mg of chitosan.

Co-delivery system and gel retardation assay

The present study described a protocol utilizing a chitosan derivative to graft ANG into the matrix of DOX-loaded PLGA NPs (Figure 2). Surface modification with cationic hydrophilic biomaterials (e.g. chitosan [31], PEI [32]) is a good strategy to make the drug delivery system positive. Thus, positively charged PLGA NPs could load negatively charged nucleic acid molecules (e.g. plasmid DNA or siRNA) by electrostatic attraction. The surface modification in our system may be achieved by hydrophobic interactions between the chitosan group and the PLGA NPs apart from the physical packaging of the chitosan group in the matrix. This

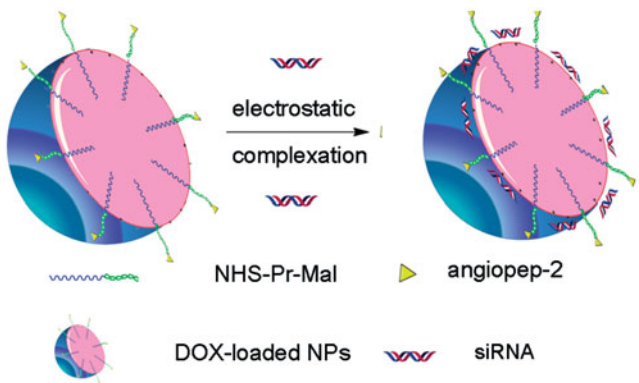

Figure 2. Formulation of co-delivery system of siRNA and doxorubicin.

modification gave rise to the positive zeta potential, which is beneficial to siRNA loading.

As shown in Figure 3, the gel retardation assay showed that EGFR siRNA could be efficiently compacted by ANG/PLGA/DOX NPs at the mass ratio of NPs to siRNA of greater than 90:1. Therefore, the specified ratio of 90:1 was used in the following experiments.

Preparation and characterization of DOX-loaded NPs

The appearance of ANG/PLGA/DOX NPs was red due to the DOX color (Figure 4A). Although DOX hydrochloride is a hydrophilic drug, the encapsulation efficiency of DOX in ANG/PLGA/DOX NPs/siRNA still could reach $75.2 \pm 3.9\%$. This result was similar to that observed for DOX-loaded PLGA NPs coated with BSA, which was reported in the literature [23].

As shown in Figure 4(B), the NPs were round and the average size was about 190 nm, which was consistent with the result of size distribution (Figure 4C). The averaged zeta potential was 38.6 ± 4.1 mV (Figure 4D), which was beneficial to deliver negatively charged siRNA.

The other three types of NPs that encapsulated DOX or simultaneously encapsulated siRNA and DOX were also prepared and characterized (Supplementary Table S1). The NPs displayed uniform size distribution and positive zeta potential. The average diameters for all NPs were similar in a range of 150–200 nm with a PDI of less than 0.250. The positive zeta potential of all NPs was provided by chitosan, which has positive group. In addition, the zeta-potentials of both siRNA- and DOX-loaded NPs were smaller than that of the corresponding DOX-loaded NPs, indicating the adsorption of siRNA on the NP surface.

In vitro drug release

As reported in previous studies, DOX release was usually evaluated in PBS buffer so as to mimic the *in vivo* biological environment [33,34]. Thus, in this study, the release profiles of DOX-loaded PLGA NPs and DOX solution *in vitro* were obtained in pH 7.4 PBS at 37 °C.

As can be seen in Figure 5(A), the drug was released fairly rapidly in DOX solution. Within 30 min, more than 30% DOX was released from DOX solution. The nonlinear fitting results are also shown in Figure 5(B) and (C), indicating that both targeting NPs with ANG (ANG/PLGA/DOX NPs) and non-targeting NPs without ANG (NANG/PLGA/DOX NPs) displayed the similar biphasic release profile with a slight burst release effect. For free DOX, the percentage of free drug hardly reached up to 30% at 1 h.

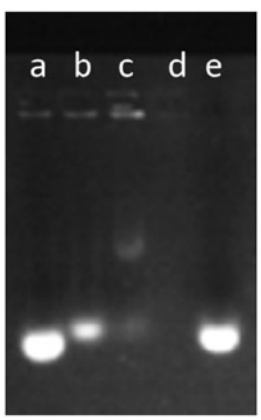

Figure 3. Electropherogram of ANG/PLGA/DOX/siRNA NPs at different weight ratio of ANG/PLGA/DOX NPs to siRNA: (a) 15:1; (b) 30:1; (c) 90:1; (d) ANG/PLGG/DOX NPs alone and (e) siRNA alone.

Thermal analysis

DSC was implemented to study the physical state of DOX in NPs. Figure 5(D) shows the DSC curves of blank ANG/PLGA NPs, ANG/PLGA/DOX NPs, pure PLGA, pure DOX and a mixture of DOX and blank ANG/PLGA NPs, respectively. The glass transition temperature (T_g) of pure PLGA was around at 48 °C, which was in agreement with the reported T_g of PLGA in the literature [35]. DOX had a melting point around 209 °C standing for an exothermic peak, which could be owing to crystallization. Besides, a melting point around 240 °C presented as endothermic peak was attributed to decomposition. However, the absence of the characteristic melting point peaks of DOX in ANG/PLGA/DOX NPs may result from the encapsulation process since the peaks could be seen in the mixture of blank ANG/PLGA NP and DOX. Therefore, it could be concluded that DOX in the NPs might exist in the amorphous phase. Therefore, the encapsulation process might interfere with the formation of drug crystals, which brought benefit to keep drug stability in NPs. The slight shift in the corresponding peak positions of T_g of PLGA in ANG/PLGA and ANG/PLGA/DOX may be ascribed to the *Van der Waals* interaction between the drug and the materials.

Cellular uptake

In our previous study, siRNA alone could not be transfected into cells without the help of drug delivery system [26,27]. Confocal images in Figure 6(A) and (B) revealed that the DOX-fluorescence (red) and siRNA-fluorescence (green) co-existed in the U87MG cells. Overlapping of red and green fluorescence of the cells transfected with the co-delivery system generated brown staining in the merged images. Compared to the non-targeting NPs (NANG/PLGA/DOX/siRNA NPs), the targeting one (ANG/PLGA/DOX/siRNA NPs) entered the cells much more efficiently, leading to a significantly intensified intracellular fluorescence. Therefore, these images confirmed that siRNA and DOX were simultaneously delivered into U87MG cells by the NPs. Furthermore, as shown in Figure 6(C) and (D), flow cytometric analysis demonstrated that the percentage of DOX-positive cells and siRNA-positive cells of ANG/PLGA/DOX/siRNA NPs group was significantly higher than that of NANG/PLGA/DOX/siRNA group. These results may be due to the surface modification of the NPs. Firstly, chitosan-coated NPs exhibited positive property, which could easily adhere to cell membranes through non-specific electrostatic interaction. Secondly, ANG could not only recognize and bind to the LPR1 on the U87MG cells mediating receptor-mediated endocytosis, but also is a P-glycoprotein inhibitor [19,20], which could retain more DOX and siRNA in the tumor cells.

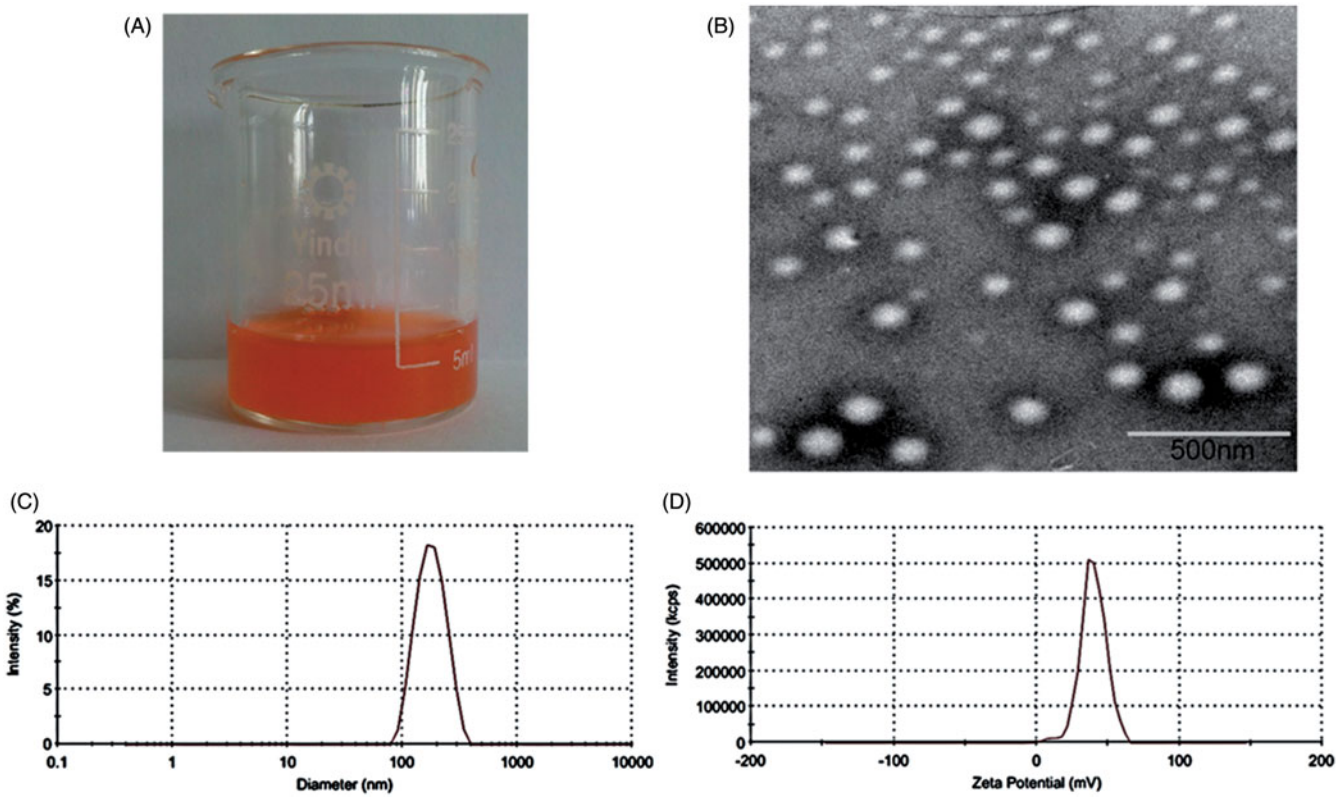

Figure 4. Characterization of ANG/PLGA/DOX/siRNA. (A) Photo of ANG/PLGA/DOX/siRNA NPs in water; (B) TEM picture of ANG/PLGA/DOX/siRNA; (C) Size distribution of ANG/PLGA/DOX/siRNA NPs; (D) Zeta potential distribution of ANG/PLGA/siRNA NPs.

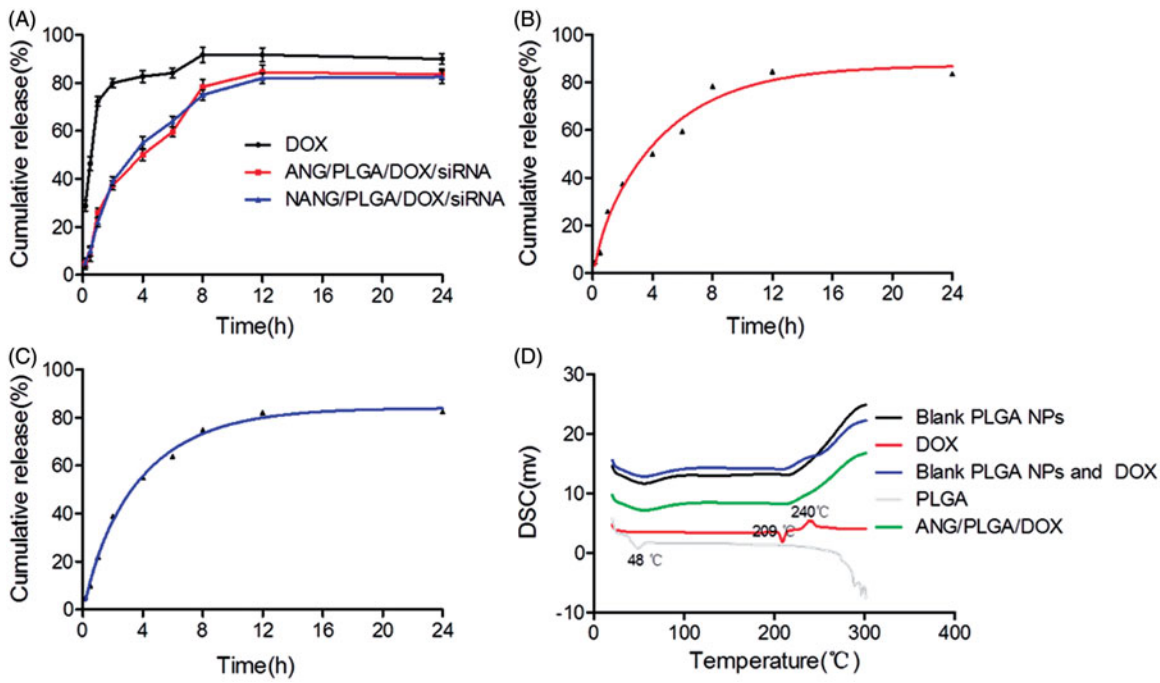

Figure 5. DOX release profiles *in vitro*, DSC curves, schematic illustration of the co-delivery system and electropherogram profile. (A) DOX release profiles of ANG/PLGA/DOX NPs, NANG/PLGA/DOX NPs and DOX solution; (B) Nonlinear fitting curve of the release profile of ANG/PLGA/DOX NPs; (C) Nonlinear fitting curve of the release profile of NANG/PLGA/DOX NPs; (D) DSC curves of pure PLGA, pure DOX, ANG/PLGA/DOX NPs, physical mixture of DOX and blank PLGA NPs (1:8), and blank PLGA NPs.

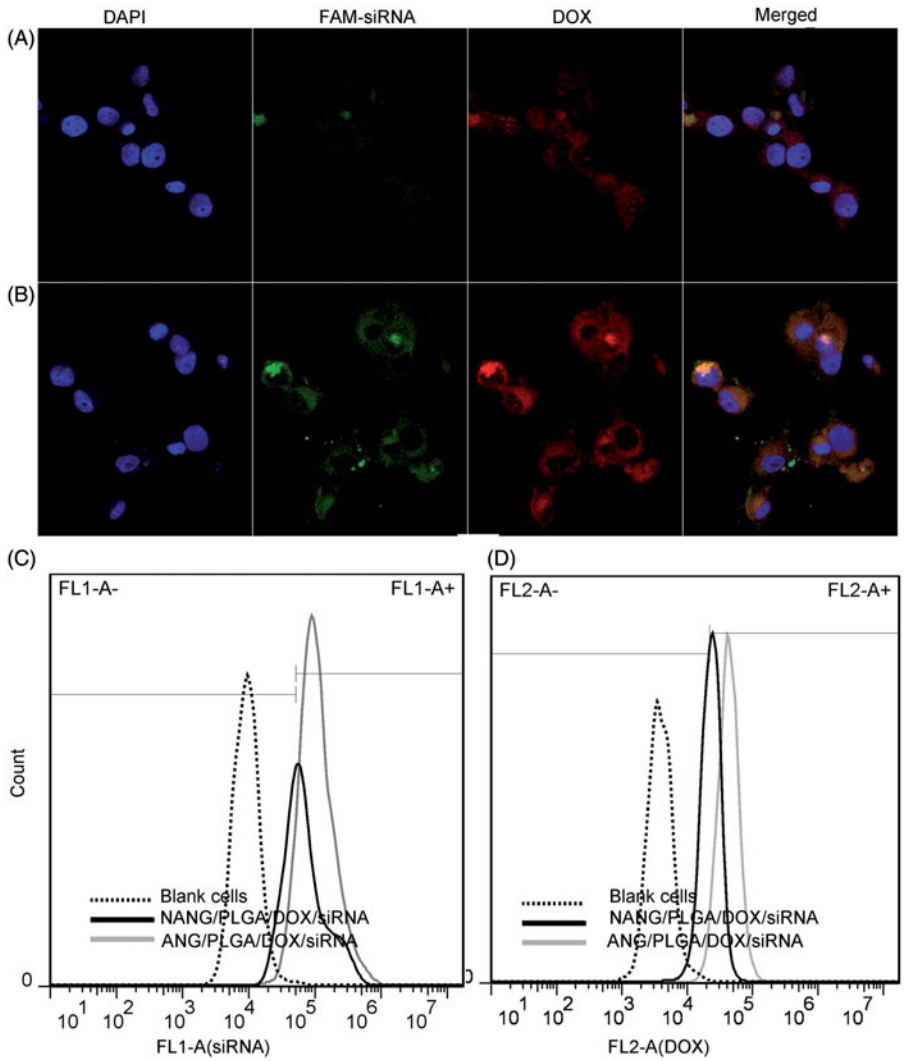

Figure 6. Quantitative and qualitative study of drug system uptake by U87MG cells. (A) Confocal microscopic images of cells treated with NANG/PLGA/DOX/siRNA after 4 h incubation; (400×). (B) Confocal microscopic images of cells treated with ANG/PLGA/DOX/siRNA after 4 h incubation; (400×). (C) Quantitative determination of FAM-siRNA-positive cells by flow cytometry. (D) Quantitative determination of DOX-positive cells by flow cytometry. (For interpretation of the references to colour in this figure legend, the reader is referred to the web version of this article.)

Analysis of combination effects

The results in Figure 7(A) indicated that ANG/PLGA NPs had no significant cytotoxicity to U87MG cells even when the concentration reached 100 μg/mL, suggesting the biocompatibility of the drug carrier itself.

Figure 7(B) and (C) shows the cytotoxicity of the drug-loaded PLGA NPs and free drug at different DOX concentrations toward U87MG cells. Free DOX cannot remarkably inhibit cell growth (less than 50%) at 24 h. Although the incubation time reached 48 h, the inhibition rate was no more than 60%. Similar results were also reported by others [36]. The relatively low cell inhibition rate of free DOX could be explained by the insensitivity of U87 cells to the drug. It has been reported that U87MG cells are not very sensitive to DOX because they are refractory to chemotherapy due to over-expression of P-glycoprotein [37]. Interestingly, as shown in Figure 7(C) and (D), when U87MG cells were exposed to an equivalent DOX concentration of DOX-loaded PLGA NPs for 48 h, marked cell inhibition was observed. Meanwhile, the targeting NPs with ANG exhibited a stronger inhibitory effect than the non-targeting NPs without ANG. Moreover, the combination formulation of either ANG/PLGA/DOX/siRNA or NANG/PLGA/DOX/siRNA caused a more significant increase in cell inhibition compared to DOX-loaded NPs (either ANG/PLGA/DOX or NANG/PLGA/DOX). As expected, the combination formulation with the targeting ligand ANG (ANG/PLGA/DOX/siRNA) caused a more significant inhibitory effect than the combination formulation without the targeting ligand (NANG/PLGA/DOX/siRNA), which could be strongly attributed to the function of ANG.

The enhanced effect of the combination formulation also emerged in the cell apoptosis test. In our previous study, free siRNA could not induce cell apoptosis obviously [26,27]. In this study, the same result was also obtained (data was not shown). As shown in Figure 8(A), cell apoptosis was detected in the presence of DOX-loaded NPs, EGFR siRNA-loaded NPs or a combination formulation of DOX and EGFR siRNA for 24 h. Compared to either DOX- or siRNA-loaded NPs, the combination formulations caused a more severe cell apoptosis with an apoptosis ratio of $30.10 \pm 3.4\%$ and $38.40 \pm 2.9\%$ for NANG/PLGA/DOX/siRNA NPs and ANG/PLGA/DOX/siRNA NPs, respectively. This indicated that the targeting NPs with ANG had a more significant effect on cell apoptosis, which further confirmed the affection of the targeting peptide.

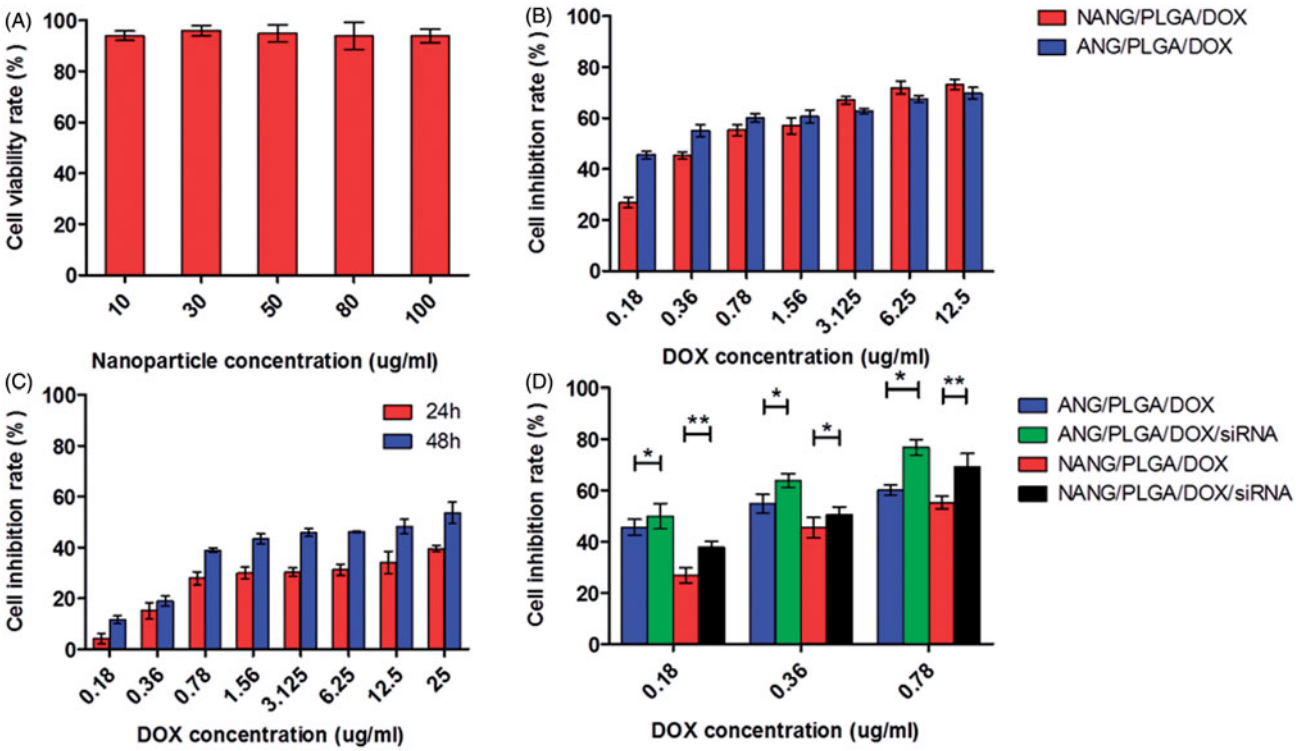

Figure 7. U87MG cell inhibition rate detected by SRB assay. (A) Cytotoxicity of blank ANG/PLGA NPs; (B) Cell inhibition in the presence of free DOX at different concentrations for 24 and 48 h. (C) Cell inhibition in the presence of ANG/PLGA/DOX and NANG/PLGA/DOX NPs for 48 h. (D) Combination inhibitory effect of DOX-loaded PLGA NPs with or without siRNA at 48 h (siRNA concentration was set at 50 nM). $*p<0.05$, $**p<0.01$. Note: Data are presented as mean ± S.D. ($n=3$).

Delivery system reduced hEGFR expression level in U87MG cells

The effects of NANG/PLGA/DOX/siRNA and ANG/PLGA/DOX/siRNA on hEGFR expression were assayed by qRT-PCR. qRT-PCR results showed that hEGFR mRNA expression in U87MG cells was significantly reduced by transfection of both types of NPs loaded with hEGFR siRNA (i.e. NANG/PLGA/DOX/siRNA, ANG/PLGA/DOX/siRNA), with a percentage of the control of 57.6 ± 7.2% and 32.4 ± 6.8%, respectively (Figure 8B). In addition, targeted NPs without hEGFR siRNA (i.e. ANG/PLGA/DOX) did not downregulate EGFR expression, indicating that this hEGFR downregulation is specifically related to the EGFR siRNA. This result is consistent with the previous results confirming that ANG-modified PLGA NPs possess an excellent capability of entering cancer cells and delivering siRNA.

Brain delivery

Coumarin-6 had been exploited for *in vivo* tracking, cellular uptake and intracellular transfer mechanism investigation on drug delivery systems [38]. We studied the brain uptake of the NPs labelled with coumarin-6 in mice at 1, 2 and 3 h after intravenous injection by fluorescence microscopy. The fluorescence signals were hardly observed in the brain tissues collected from the mice intravenously administrated with the non-targeting NPs (NANG/PLGA/Coumarin-6 NPs) and coumarin-6 solution (Supplementary Figures S1 and S2). More punctate fluorescence around the nuclei and relatively stronger fluorescence were observed in the brain striatum collected from the mice intravenously administrated with the

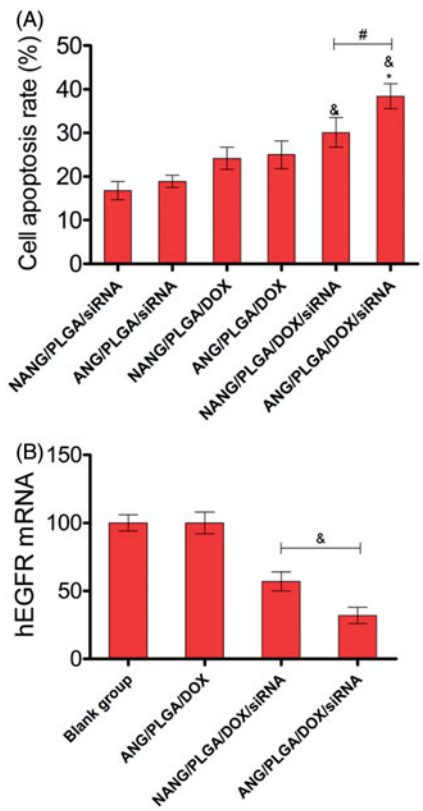

Figure 8. Apoptosis ratio of U87MG cells treated with different drug systems for 24 h. $*p<0.05$ versus siRNA-loaded NPs, $\&p<0.01$ versus DOX-loaded NPs, $\#p<0.01$. Note: Data are presented as mean ± S.D. ($n=3$). The DOX concentration was set as 0.36 μg/mL and the siRNA concentration was set as 50 nM.

non-targeting NPs than coumarin-6 solution, which may be attributed to the non-specific electrostatic effect between the positive NPs and brain capillary endothelial cells. However, the targeting NPs (ANG/PLGA/Coumarin-6 NPs) showed strong ability to deliver drug into the brain, leading to significantly intensified green punctate fluorescence around the nuclei (Figure 9). Therefore, we believe that the green punctate fluorescence observed were mainly associated with the NPs. Moreover, the fluorescence became much brighter at 3 h after drug injection (Figure 9C). As shown in Figure 9(D), higher magnification images further revealed the distribution of the NPs in the cytoplasm as well as in periphery of the nuclei. These data suggested that the ANG/PLGA NPs could successfully penetrate the BBB and serve as a brain drug delivery system to deliver therapeutic agents for glioma therapy, which was dependent on the brain targeting peptide.

Pharmacokinetics and biodistribution

The different pharmacokinetic parameters of DOX-loaded PLGA NPs and DOX solution when administered by intravenous route were calculated by determining the concentration of DOX in plasma and tissue homogenate. The DOX concentrations in plasma at different times are shown in Figure 10(A).

As can be seen in Table 1, the AUCs of both DOX-loaded NPs were higher than those of the DOX solution with a 1.53- and 1.59-fold increase for ANG/PLGA/DOX NPs and NANG/PLGA/DOX, respectively. The clearance of ANG/PLGA/DOX, NANG/PLGA/DOX NPs and DOX was 1.130, 1.145 and 2.857 (mg/kg)/(μg/mL)/h, respectively. These findings might be explained by the sustained-release profile of DOX-loaded NPs, which is consistent with the *in vitro* results. It was reported that the mass of drug delivered to the brain is

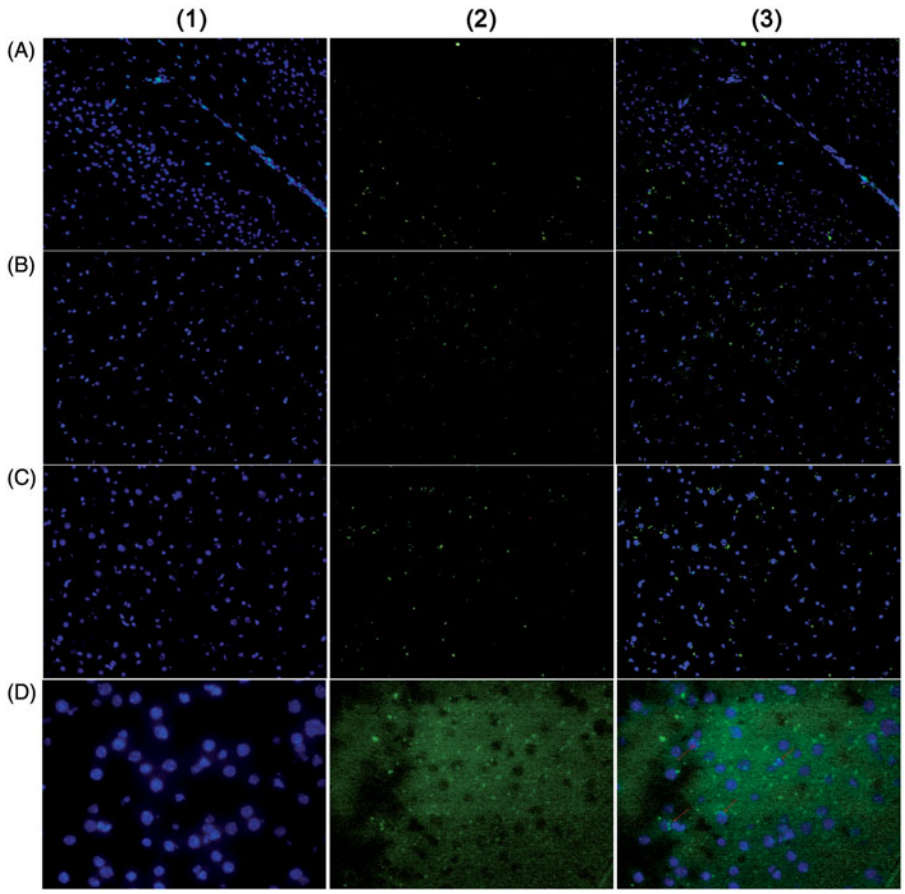

Figure 9. Representative fluorescence microscopic images of the brain tissues from mice treated intravenously with targeting NPs labelled with coumarin-6 (ANG/PLGA/Coumarin-6 NPs/siRNA). (A) 1 h (200×); (B) 2 h (200×); (C) 3 h (200×); (D) 3 h (400×). Column (1): The nuclei in blue fluorescence are stained with DAPI. Column (2): Fluorescein isothiocyanate channels showing the green fluorescence from coumarin-6-loaded PLGA NPs distributed in brain tissues. Column (3): Merged channel of fluorescein isothiocyanate and DAPI. (For interpretation of the references to colour in this figure legend, the reader is referred to the web version of this article.)

Table 1. The pharmacokinetic parameters of DOX after intravenous administration of DOX, ANG/PLGA/DOX and NANG/PLGA/DOX in mice.

Parameter	Unit	ANG/PLGA/DOX	NANG/PLGA/DOX	DOX
$t_{1/2}$	h	1.431	1.655	1.843
AUC_{0-t}	μg/mL h	2.061	1.965	0.783
AUC_{0-inf_obs}	μg/mL h	2.653	2.618	1.049
$AUMC_{0-inf\_obs}$	μg/mL h^2	5.006	5.477	2.205
MRT_{0-inf_obs}	h	1.886	2.092	2.100
$Cl_{\_obs}$	(mg/kg)/(μg/mL)/h	1.130	1.145	2.857
$Vss_{\_obs}$	(mg/kg)/(μg/mL)	2.133	2.397	6.003

All data are the average of three measurements.

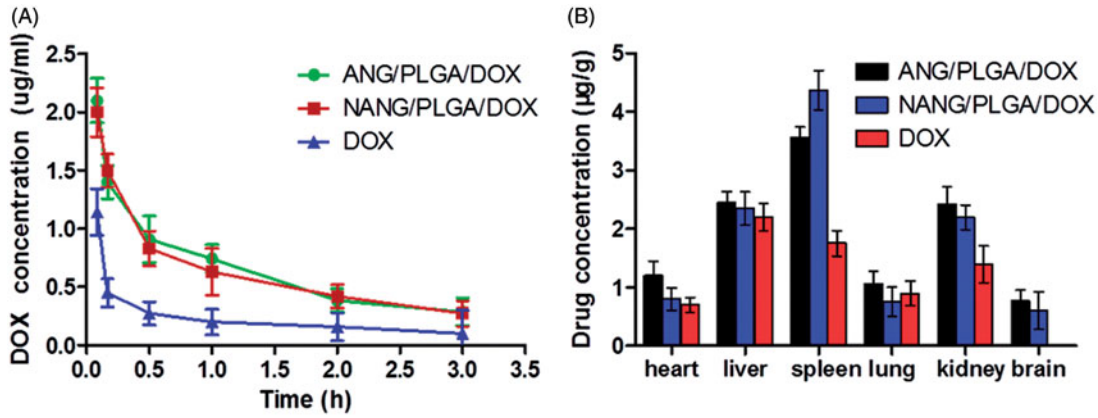

Figure 10. Mean DOX concentration in plasma at different times after intravenous administration of DOX, ANG/PLGA/DOX and NANG/PLGA/DOX and biodistribution in mice at 3 h after injection (i.v.). Data are presented as mean ± S.D. ($n = 6$).

equally proportional to the BBB permeability coefficient and the areas under curve plasma concentration versus time (AUC) [39]. Therefore, optimal chemical and physical properties of the NPs decreased the plasma clearance of DOX in the circulation and increased the possibility to cross the BBB. However, it is important to note that the mean residence time between each group was not significantly different, which can be attributed to the positive surface charge of the NPs. The literature [40] demonstrated that NPs with high positive charge (>10 mV) were efficiently opsonized and cleared by the Kupffer cells from the blood circulation.

As shown in Figure 10(B), overall there was a relatively high distribution in liver, spleen and probably because of the sessile macrophages present there [41]. In the brain, the drug concentration at 3 h for the ANG/PLGA/DOX and NANG/PLGA/DOX were 0.78 ± 0.12 and 0.60 ± 0.32 μg/mL, respectively, while DOX can hardly be detected in the brain for the free DOX solution group at 3 h, indicating that DOX-loaded NPs provided a higher drug concentration in the brain in comparison to the DOX solution. These data further confirmed that the ANG-modified PLGA NPs could effectively deliver the drug into the brain. These NPs transport may be mediated by receptor-mediated transcytosis due to the existence of corresponding receptor of ANG expressed on the endothelia cells. In addition, the electrostatic interaction between the positive NPs and negative endothelia cells also contributed to the accumulation of NPs in the brain because the non-targeting system (NANG/PLGA/DOX) also showed more delivery of drug to the brain.

In vivo anti-glioma efficacy

Xenografting of human cancer cell lines injected subcutaneously in nude mice has become the common testing platform for dissecting mechanistic aspects of tumorigenesis and for pre-clinical drug research. However, subcutaneous xenografts do not represent tumors in their tissue of origin and thus may have some clinically relevant deficiency. Xenografted human tumor cells directly injected into their relevant organ may present a more accurate model of human tumors. So we established the orthotopic mouse xenograft model of glioma for evaluating the anti-glioma efficacy of drug-loaded NPs. The survival of the animal was monitored and recorded daily, which are presented in Figure 11(A). The median survival time (MST) of saline group, DOX group, NANG/PLGA/DOX group, ANG/PLGA/DOX group, NANG/PLGA/DOX/PLGA/siRNA and ANG/PLGA/DOX/siRNA were 27.3, 31.0, 32.8, 39.5, 45.0, 47.8 days, respectively (Table 2). Although ANG/PLGA/DOX/siRNA could not thoroughly cure the glioma-bearing mice, the increased time survival time of ANG/PLGA/DOX/siRNA compared to ANG/PLGA/DOX, DOX and saline were as long as 8.3, 16.8 and 20.5 days, respectively. However, the mice treated with ANG/PLGA/DOX/siRNA showed no significant different MST compared to mice treated with NANG/PLGA/DOX/siRNA. It is well known that NPs tend to accumulate in tumors due to the enhanced permeability and retention effect. This should explain the reasons why all the formulations including the NPs without the targeting peptide showed anti-tumor activity compared to the saline group. With the help of the targeting peptide, ANG/PLGA/DOX certainly showed better efficacy with longer MST than NANG/PLGA/DOX. It is reasonable that the formulation of NANG/PLGA/DOX/siRNA showed longer MST compared to the NANG/PLGA/DOX group due to the additional effect of the siRNA. However, further addition of the targeting peptide ANG to the NPs (ANG/PLGA/DOX/siRNA) failed to further prolong the MST probably due to the almost saturated anti-tumor effect caused by NANG/PLGA/DOX/siRNA. Therefore, it is not surprising to find that the difference between ANG/PLGA/DOX/siRNA and NANG/PLGA/DOX/siRNA is less when compared to ANG/PLGA/DOX and NANG/PLGA/DOX. Thus, the multifunctional ANG-modified PLGA NPs encapsulated both DOX and EGFR siRNA demonstrated to be a promising drug delivery system for glioma therapy.

The representative Nissl-stained coronal sections from the same location of the brain from untreated mice and the mice receiving different formulations at 25 days are displayed in Figure 11(B). The glioma of mice treated with saline had poorly defined borders due to the invasion of normal brain tissue. The glioma volume decreased after the treatment with drug-loaded NPs, suggesting that the NPs could deliver more drugs to the glioma. It was reported that the over-expression

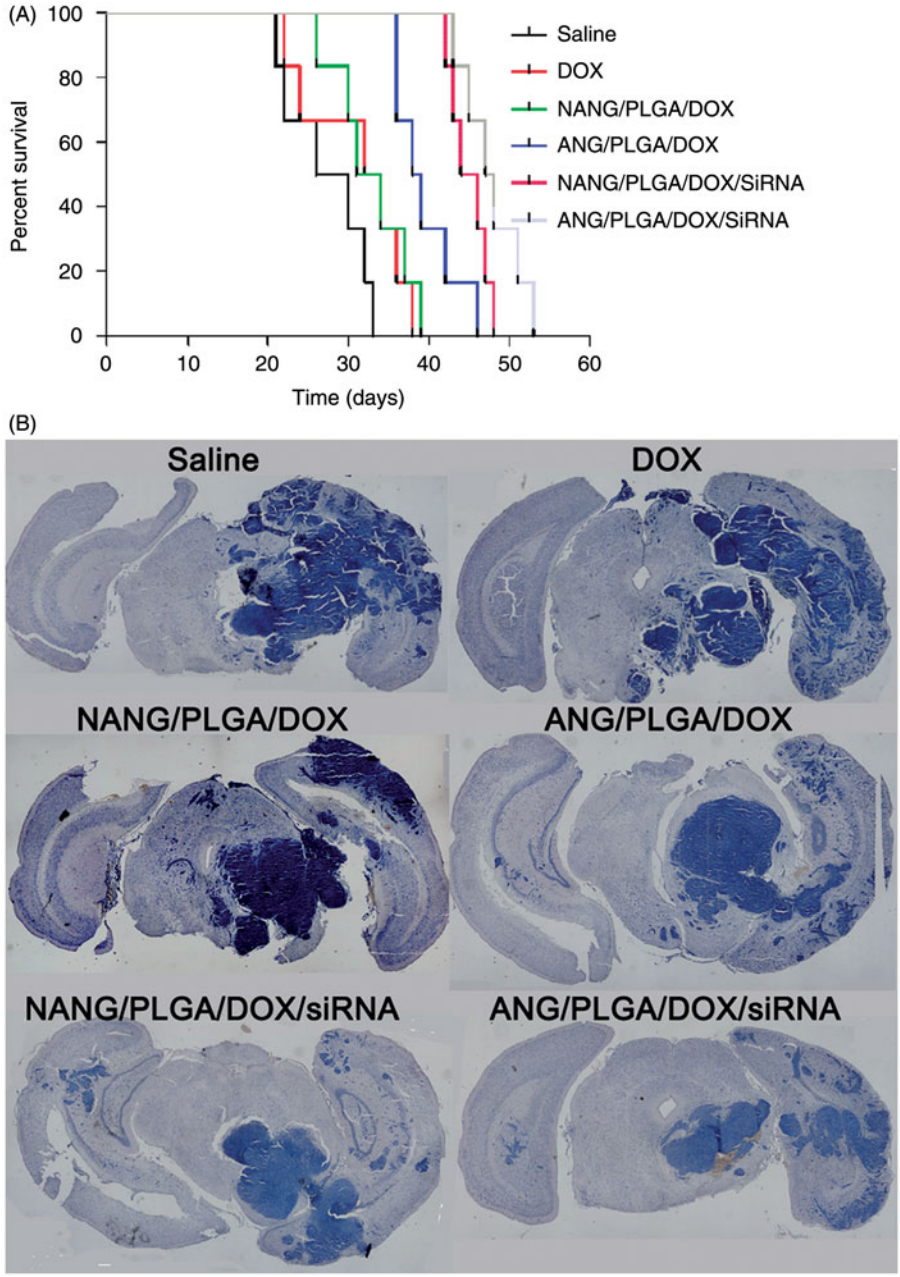

Figure 11. Survival curves of U87MG glioma bearing mice and photographs showing the appearance of representative brain tumor sections stained with Nissl. (A) Kaplan–Meier survival curves of U87MG glioma bearing Balb/c mice ($n = 6$); (B) Photographs of Nissl-stained brain tissue from intracranial U87MG glioma-bearing mice after intravenous administration of drug-loaded NPs. After 25 days of the treatment, brain tissues were taken from all the groups.

Table 2. Median survival time of mice bearing intracranial U87MG glioma treated with different formulations.

Treatment	Number of mice	Median survival time	Standard error	*p* Value
Saline	6	27.3	2.1	
DOX	6	31.0	2.7	>0.05[a]
NANG/PLGA/DOX	6	32.8	2.0	>0.05[a]
ANG/PLGA/DOX	6	39.5	1.6	<0.05[a,b]
NANG/PLGA/DOX/siRNA	6	45.0	1.0	<0.01[a,b]
ANG/PLGA/DOX/siRNA	6	47.8	1.5	<0.01[a,c]

[a]Compared to saline.
[b]Compared to NANG/PLGA/DOX.
[c]Compared to ANG/PLGA/DOX.

of EGFR is associated with the invasion of glioma [42,43]. Therefore, suppressing tumor growth and invasion are equally important for glioma therapy. The glioma size was the lowest after the treatment with ANG/PLGA/DOX/siRNA, indicating that combination therapy markedly suppressed tumor growth and invasion.

In order to investigate the glioma suppression mechanism, TUNEL assay was carried out to investigate apoptosis level in

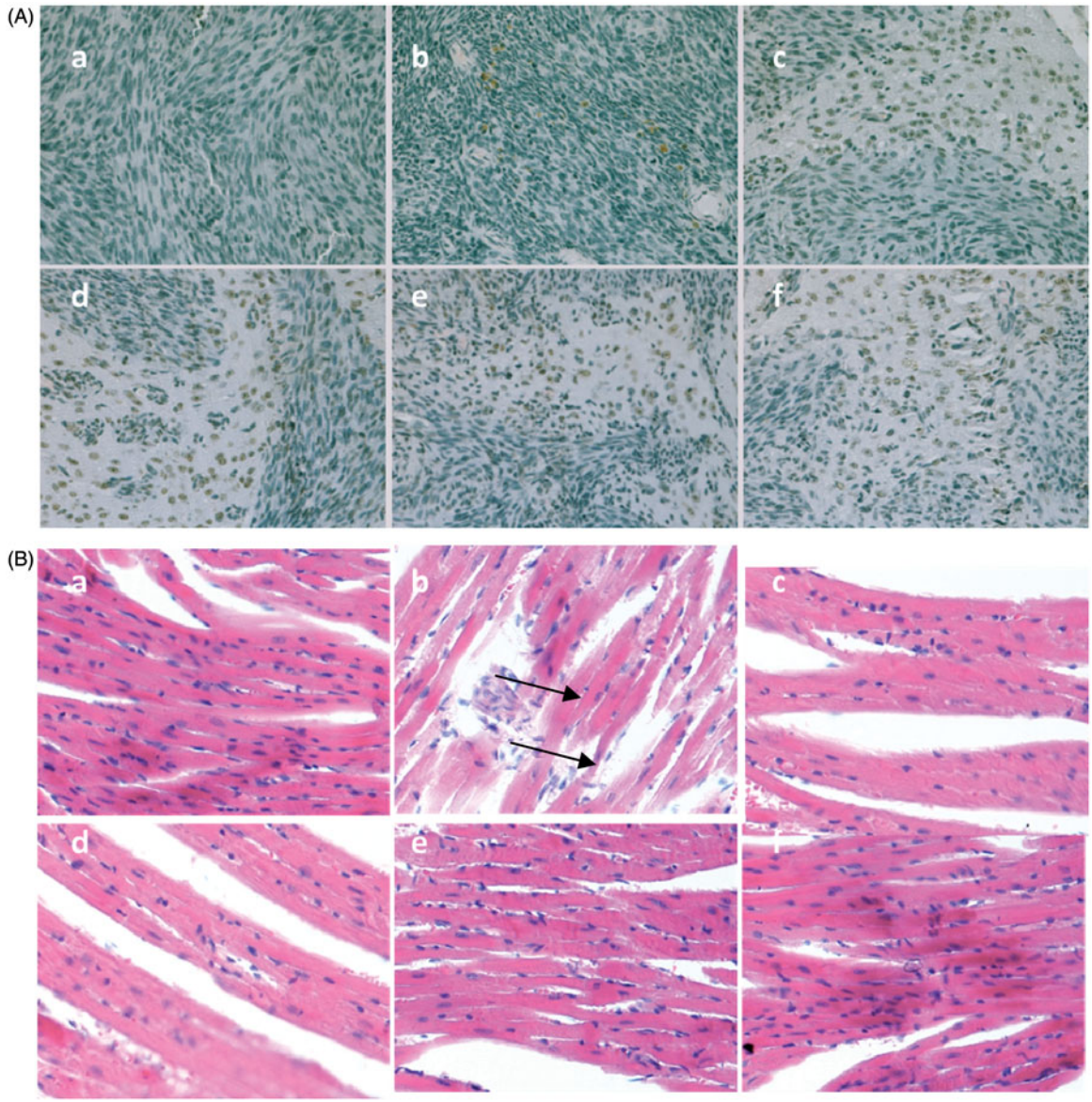

Figure 12. Tumor apoptosis and toxicity evaluation. (A) Images of tumor apoptosis detected by TUNEL assay after 25 days of the treatment. (B) Histochemistry analysis of heart section stained with hematoxylin and eosin of mice bearing glioma after 25 days of the treatment. (a) Saline; (b) DOX; (c) NANG/PLGA/DOX; (d) ANG/PLGA/DOX; (e) NANG/PLGA/DOX/siRNA; (f) ANG/PLGA/DOX/siRNA. Images were acquired under a fluorescence microscope with a 20× objective lens. Arrow: muscle fiber breakage and cell nucleus gather.

glioma from mice treated with different formulations. The results revealed that apoptotic nuclei were stained dark brown while normal nuclei were stained blue [44]. As shown in Figure 12(A), for mice treated with NAG/PLGA/DOX, ANG/PLGA/DOX, NANG/PLGA/DOX/siRNA, significant apoptotic response of glioma cells and wider cell gap of glioma tissue were obviously observed. What's more, much more apoptotic glioma cells in ANG/PLGA/DOX/siRNA glioma tissues were detected in comparison with any other treatment. Nevertheless, less obvious glioma apoptosis was also observed in free DOX group in comparison with the saline group. Thus, the increased cell apoptosis induced by DOX and EGFR siRNA may contribute to the decreased tumor size, which further prolonged the survival time of U87MG glioma bearing Balb/c mice.

The H&E staining for the heart section from DOX-loaded NPa showed that there is no evidence of abnormal and inflammatory cell infiltration in heart sections, indicating DOX-loaded NPs does cause toxicity on heart of the mice. However, in the DOX solution, muscle fiber breakage and cell nucleus gather were observed.

Conclusion

In this research project, a NP-based brain-targeted drug delivery system for co-delivery of gene and chemotherapy drug was prepared and characterized. EGFR siRNA and DOX were successfully loaded in the PLGA NPs. A new chitosan derivative was synthesized to anchor the targeting ligand ANG onto the surface of the NPs. The DOX-loaded PLGA NPs exhibited a sustained release profile with diminished burst release at the initial phase. The *in vitro* cell uptake experiment showed that DOX and siRNA could be simultaneously delivered into U87MG cells efficiently by the NPs.

The combination formulation ANG/PLGA/DOX/siRNA NPs showed the strongest inhibitory and apoptotic effect on U87MG cells than any other formulations. Although U87 xenografted model is different from what is expected of a primary glioma, it also may present a more accurate model of human tumors for studying whether one certain drug delivery system could have the improved anti-glioma ability. The *in vivo* study confirmed that this drug system was able to cross the BBB and combination therapy of EGFR siRNA and DOX could remarkably prolong the survival time of U87MG glioma mice. Thus, the multifunctional ANG-modified PLGA NPs loaded with both DOX and EGFR siRNA can provide a promising approach to treat glioma.

Declaration of interest

This study was supported by the National Natural Science Foundation of China under grant Nos. 81272527 and 81302717.

References

1. Bicker J, Alves G, Fortuna A, Falcao A. Blood-brain barrier models and their relevance for a successful development of CNS drug delivery systems: a review. Eur J Pharm Biopharm 2014;87:409–32.
2. Krol S. Challenges in drug delivery to the brain: nature is against us. J Control Release 2012;164:145–55.
3. Amoozgar Z, Wang L, Brandstoetter T, et al. Dual-layer surface coating of PLGA-based nanoparticles provides slow-release drug delivery to achieve metronomic therapy in a paclitaxel-resistant murine ovarian cancer model. Biomacromolecules 2014;15:4187–94.
4. Mo L, Hou L, Guo D, et al. Preparation and characterization of teniposide PLGA nanoparticles and their uptake in human glioblastoma U87MG cells. Int J Pharm 2012;436:815–24.
5. Danhier F, Ansorena E, Silva JM, et al. PLGA-based nanoparticles: an overview of biomedical applications. J Control Release 2012;161:505–22.
6. Zarschler K, Prapainop K, Mahon E, et al. Diagnostic nanoparticle targeting of the EGF-receptor in complex biological conditions using single-domain antibodies. Nanoscale 2014;6:6046–56.
7. Zhang Y, Zhang YF, Bryant J, et al. Intravenous RNA interference gene therapy targeting the human epidermal growth factor receptor prolongs survival in intracranial brain cancer. Clin Cancer Res 2004;10:3667–77.
8. Pushparaj PN, Melendez AJ. Short interfering RNA (siRNA) as a novel therapeutic. Clin Exp Pharmacol Physiol 2006;33:504–10.
9. de Fougerolles A, Vornlocher HP, Maraganore J, Lieberman J. Interfering with disease: a progress report on siRNA-based therapeutics. Nat Rev Drug Discov 2007;6:443–53.
10. Khan M, Ong ZY, Wiradharma N, et al. Advanced materials for co-delivery of drugs and genes in cancer therapy. Adv Healthc Mater 2012;1:373–92.
11. Liu S, Guo Y, Huang R, et al. Gene and doxorubicin co-delivery system for targeting therapy of glioma. Biomaterials 2012;33:4907–16.
12. Mignani S, Bryszewska M, Klajnert-Maculewicz B, et al. Advances in combination therapies based on nanoparticles for efficacious cancer treatment: an analytical report. Biomacromolecules 2014;16:1–27.
13. Huang HY, Kuo WT, Chou MJ, Huang YY. Co-delivery of anti-vascular endothelial growth factor siRNA and doxorubicin by multifunctional polymeric micelle for tumor growth suppression. J Biomed Mater Res Part A 2011;97A:330–8.
14. Liu CW, Lin WJ. Using doxorubicin and siRNA-loaded heptapeptide-conjugated nanoparticles to enhance chemosensitization in epidermal growth factor receptor high-expressed breast cancer cells. J Drug Target 2013;21:776–86.
15. Skandrani N, Barras A, Legrand D, et al. Lipid nanocapsules functionalized with polyethyleneimine for plasmid DNA and drug co-delivery and cell imaging. Nanoscale 2014;6:7379–90.
16. Wang H, Su W, Wang S, et al. Smart multifunctional core-shell nanospheres with drug and gene co-loaded for enhancing the therapeutic effect in a rat intracranial tumor model. Nanoscale 2012;4:6501–8.
17. Presumey J, Salzano G, Courties G, et al. PLGA microspheres encapsulating siRNA anti-TNFalpha: efficient RNAi-mediated treatment of arthritic joints. Eur J Pharm Biopharm 2012;82:457–64.
18. Yuan X, Shah BA, Kotadia NK, et al. The development and mechanism studies of cationic chitosan-modified biodegradable PLGA nanoparticles for efficient siRNA drug delivery. Pharm Res 2010;27:1285–95.
19. Demeule M, Currie JC, Bertrand Y, et al. Involvement of the low-density lipoprotein receptor-related protein in the transcytosis of the brain delivery vector Angiopep-2. J Neurochem 2008;106:1534–44.
20. Demeule M, Regina A, Che C, et al. Identification and design of peptides as a new drug delivery system for the brain. J Pharmacol Exp Ther 2008;324:1064–72.
21. Maletinska L, Blakely EA, Bjornstad KA, et al. Human glioblastoma cell lines: levels of low-density lipoprotein receptor and low-density lipoprotein receptor-related protein. Cancer Res 2000;60:2300–3.
22. Drappatz J, Brenner A, Wong ET, et al. Phase I study of GRN1005 in recurrent malignant glioma. Clin Cancer Res 2013;19:1567–76.
23. Betancourt T, Brown B, Brannon-Peppas L. Doxorubicin-loaded PLGA nanoparticles by nanoprecipitation: preparation, characterization and in vitro evaluation. Nanomedicine (Lond) 2007;2:219–32.
24. Cao N, Cheng D, Zou S, et al. The synergistic effect of hierarchical assemblies of siRNA and chemotherapeutic drugs co-delivered into hepatic cancer cells. Biomaterials 2011;32:2222–32.
25. Livak KJ, Schmittgen TD. Analysis of relative gene expression data using real-time quantitative PCR and the 2(-Delta Delta C(T)) method. Methods 2001;25:402–8.
26. Wang L, Shi JJ, Jia X, et al. NIR-/pH-responsive drug delivery of functionalized single-walled carbon nanotubes for potential application in cancer chemo-photothermal therapy. Pharmaceut Res 2013;30:2757–71.
27. Wang L, Shi J, Zhang H, et al. Synergistic anticancer effect of RNAi and photothermal therapy mediated by functionalized single-walled carbon nanotubes. Biomaterials 2013;34:262–74.
28. Jiang X, Dai H, Leong KW, et al. Chitosan-g-PEG/DNA complexes deliver gene to the rat liver via intrabiliary and intraportal infusions. J Gene Med 2006;8:477–87.
29. Yang F, Huang W, Li Y, et al. Anti-tumor effects in mice induced by survivin-targeted siRNA delivered through polysaccharide nanoparticles. Biomaterials 2013;34:5689–99.
30. Chan P, Kurisawa M, Chung JE, Yang YY. Synthesis and characterization of chitosan-g-poly(ethylene glycol)-folate as a non-viral carrier for tumor-targeted gene delivery. Biomaterials 2007;28:540–9.
31. Chen H, Yang W, Chen H, et al. Surface modification of mitoxantrone-loaded PLGA nanospheres with chitosan. Colloids Surf B Biointerfaces 2009;73:212–18.
32. Wong K, Sun G, Zhang X, et al. PEI-g-chitosan, a novel gene delivery system with transfection efficiency comparable to polyethylenimine in vitro and after liver administration in vivo. Bioconjug Chem 2006;17:152–8.
33. Lin R, Shi NL, Wang CH. In vitro study of anticancer drug doxorubicin in PLGA-based microparticles. Biomaterials 2005;26:4476–85.
34. Park J, Fong PM, Lu J, et al. PEGylated PLGA nanoparticles for the improved delivery of doxorubicin. Nanomedicine 2009;5:410–18.
35. Amjadi I, Rabiee M, Hosseini MS, Mozafari M. Synthesis and characterization of doxorubicin-loaded poly(lactide-co-glycolide) nanoparticles as a sustained-release anticancer drug delivery system. Appl Biochem Biotechnol 2012;168:1434–47.

36. Lu YJ, Wei KC, Ma CC, et al. (2012) Dual targeted delivery of doxorubicin to cancer cells using folate-conjugated magnetic multi-walled carbon nanotubes. Colloids Surf B Biointerfaces 2012;89: 1–9.
37. Kaneshiro TL, Lu Z. Targeted intracellular codelivery of chemotherapeutics and nucleic acid with a well-defined dendrimer-based nanoglobular carrier. Biomaterials 2009;30: 5660–6.
38. Guo M, Rong WT, Hou J, et al. Mechanisms of chitosan-coated poly(lactic-co-glycolic acid) nanoparticles for improving oral absorption of 7-ethyl-10-hydroxycamptothecin. Nanotechnology 2013;24:1–15.
39. Pardridge WM. Non-invasive drug delivery to the human brain using endogenous blood–brain barrier transport systems. Pharm Sci Technol Today 1999;2:49–59.
40. Xiao K, Li Y, Luo J, et al. The effect of surface charge on in vivo biodistribution of PEG-oligocholic acid based micellar nanoparticles. Biomaterials 2011;32:3435–46.
41. Patil RR, Yu J, Banerjee SR, et al. Probing in vivo trafficking of polymer/DNA micellar nanoparticles using SPECT/CT imaging. Mol Ther 2011;19:1626–35.
42. Li W, Wu C, Yao Y, et al. MUC4 modulates human glioblastoma cell proliferation and invasion by upregulating EGFR expression. Neurosci Lett 2014;566:82–7.
43. Parker JJ, Dionne KR, Massarwa R, et al. Gefitinib selectively inhibits tumor cell migration in EGFR-amplified human glioblastoma. Neuro Oncol 2013;15:1048–57.
44. Shi J, Zhang H, Wang L, et al. PEI-derivatized fullerene drug delivery using folate as a homing device targeting to tumor. Biomaterials 2013;34:251–61.

Supplementary material available online
Supplementary Table S1, Figures S1 and S2